JOURNAL GEOLOGICAL SOCIETY OF INDIA
Vol.83, June 2014, pp.625-634

GUI Based Inversion Code for Automatic Quantification of Strike Limited Listric Fault Sources and Regional Gravity Background from Observed Bouguer Gravity Anomalies

V. Chakravarthi and S. Rajeswara Sastry
Centre for Earth & Space Sciences, University of Hyderabad, Hyderabad – 500 046
Email: vcvarthi@rediffmail.com

Abstract: A method coupled with a GUI based code in JAVA is developed in the space domain to simultaneously estimate the structures of strike limited listric fault sources and regional gravity background from a set of observed Bouguer gravity anomalies. The density contrast within the hanging wall of the structure is assumed to be varying continuously with depth based on a parabolic equation. The limiting surface of the fault plane is described with an exponential function. This method is automatic in the sense that it initializes both parameters of a strike limited listric fault source and regional gravity background from a set of observed Bouguer gravity anomalies and improves them iteratively until the modeled gravity anomalies fit the observed anomalies within the specified convergence criteria. The advantage of the code is that besides generating output in both ASCII and graphical forms it displays the animated versions of (i) the changes in model geometry, (ii) variation of each model parameter and misfit with iteration number, (iii) improvements in modeled gravity anomalies, and (iv) variation of density contrast with depth. The applicability of the code is demonstrated on both synthetic and real field gravity anomalies. In case of synthetic example pseudorandom noise is added to the residual gravity anomalies of the structure prior to inversion. The noisy anomalies are then inverted for the unknown parameters presuming (i) an ideal listric fault structure bounded by an exponential limiting surface with perfect flat top and bottom surfaces, (ii) non-ideal structure with uneven top and bottom surfaces with imperfect exponential limiting surface. Further, the robustness of the algorithm is exemplified by adding both regional gravity background and pseudorandom noise to the anomalies of the structure before inversion. In all cases, the interpreted parameters of the structure closely mimic the assumed parameters. The interpretation of gravity anomalies across the master fault of the Chintalpudi sub-basin in India has yielded information that is consistent with both DSS results and drilling information. The highlight of the code is that it can be used to interpret the gravity anomalies of listric fault sources even when the profile along which the interpretation is intended fails to bisect the strike length of the structure.

Keywords: Finite strike listric fault source, Parabolic density function, Regional background, Inversion, Simultaneous estimation, JAVA.

INTRODUCTION

The primary goal of studying detailed gravity data is to provide a better understanding of the subsurface geology. Gravity method plays an important role to trace the boundaries of geological structures across which the density contrast varies significantly. For e.g., the gravity anomaly across a fault increases progressively to a maximum value over the uplifted side and low over the downthrown block because the displacement of material causes a horizontal density contrast across the fault plane. Furthermore, filling of low density sediments within the downthrown block of a fault structure creates significant density contrast across the fault plane and accordingly generate measurable gravity anomalies. Elongated and dense gravity anomaly contours between two widely spaced regions of a high and a low can be considered to represent a fault in the basement. The orientation and disposition of fault patterns can be studied on a Bouguer anomaly map from the flexures and dislocations of contours. These gravity anomalies can be analyzed quantitatively for the parameters of the fault structures after properly accounting for regional gravity background. The parameters to be estimated from a gravity profile over a fault structure are: depths to the top and bottom of a fault structure, location of the origin of the fault plane and the geometry of fault plane modeled as a function of depth.

Generally, large normal faults associated with thick sedimentary basins, such as the Gulf of Mexico, are curved in cross section and become almost flat at depths within the upper crust (Wernicke and Burchfiel, 1982; Jackson, 1987;

Janecke et al., 1998; Brady et al., 2000). Such listric fault structures form during rifting, drifting, and evolution of passive continental margins, with concomitant basinal development.

Because of the fact that the fault planes of listric fault sources are non-planar in nature (dips of fault planes become shallower with increased depth), it is often difficult to estimate the extension of fault blocks from surface observation of dip and throw of the faults and hence, major extension cannot be estimated easily by surface mapping alone (McKenzie, 1978). On the other hand, the detached rock masses on either side of listric fault planes create lateral contrasts in subsurface distribution of rock densities and accordingly generate detectable gravity anomalies across the fault planes of the structures (Chakravarthi, 2011).

Although many fault structures on continental regions possess finite strike lengths (Peirce and Lipkov, 1988) with fault planes non-planar in nature (Torizin et al., 2009), many interpretational techniques are in vogue to analyze the gravity anomalies of the structures treating them as 2D sources with fault planes described by planar surfaces. For eg., Thanassoulas et al. (1987), Murthy and Krishnamacharyulu (1990), Chen et al. (1992), Stavrev and Reid (2010) developed techniques to interpret the gravity anomalies of 2D fault structures using constant density. The fact that the density of sedimentary rocks varies with depth (Cordell, 1973; García-Abdeslem, 2000; Li, 2001; Chakravarthi, 2003; Chakravarthi and Sundararajan, 2006; Chappell and Kusznir, 2008; Pawlowski, 2008; Gimenez et al., 2009, Chakravarthi, 2010) and that the variation can be described by simple mathematical functions has prompted many researchers to use variable density models in the analysis of gravity anomalies.

In this direction, Bhaskara Rao (1985) and Bhaskara Rao et al. (1993) used quadratic and exponential density functions, Sundararajan and Ramabrahmam (1998) used a linear density function to analyze the gravity anomalies of fault structures. The above interpretational strategies, which are valid to analyze the residual gravity anomalies alone, may yield unreliable interpretations in the presence of regional gravity background. On the other hand, Chakravarthi and Sundararajan (2004), Chakravarthi (2008) developed techniques using parabolic density function (PDF) to simultaneously estimate the parameters of 2D and 2.5D fault structures and regional gravity background from a set of observed Bouguer gravity anomalies respectively. Nevertheless, the enlisted methods presume that fault planes are planar surfaces, which in reality may not be so as large dip slip faults are usually curved in cross-section (Jackson and McKenzie, 1983).

On the other hand, a few forward-modeling schemes are available to accommodate the geometries of listric fault sources to compute the gravity responses (Martín-Atienza and García-Abdeslem, 1999; Zhang et al., 2001; Zhou, 2008, 2009). Again these strategies are efficient only with 2D sources. Chakravarthi (2010) developed a method coupled with a computer program using a parabolic density function to realize forward gravity modeling of strike limited listric fault sources, wherein the fault planes are described by polynomial functions of arbitrary degree. The practical applicability of the above forward modeling schemes is also restricted because the parameters of fault structures are not known beforehand.

In recent past, García-Abdeslem (2000) developed a technique using a depth-dependent density function to analyze the gravity anomalies of geologic sources bounded laterally by continuous surfaces. This technique, being 2D, is efficient only with residual gravity anomalies. It is well-known that the observed gravity anomalies of a fault structure attains to zero and maximum magnitudes only at very large distances on either side of the fault plane, therefore it is seldom possible to precisely isolate the signal due to the structure from observed Bouguer gravity anomalies. In addition, the accuracy of interpretation by this method is also dependent on the choice of initial model parameters as demonstrated by García-Abdeslem (2000). Therefore, automatic algorithms using variable-density models are preferable to simultaneously estimate the model parameters of fault structures treated as strike-limited (2.5D) sources with fault planes described by nonplanar surfaces and regional gravity background from observed gravity anomalies.

In this direction, Chakravarthi (2011) developed an automatic inversion algorithm to model 2.5D listric fault sources from the observed Bouguer gravity anomalies, where the fault planes and regional gravity background are described by polynomial functions of arbitrary degree and the density contrast within the detached block of the structure by a parabolic function. Because the degree of polynomial to be chosen to describe the fault planes is always uncertain in the absence of additional sources of information on the subsurface, the choice of higher degree polynomials in the inversion may likely affect the numerical stability of the interpretation (Chakravarthi, 2011).

In this paper a method and an associated GUI based JAVA code (available with authors) is developed to analyze the gravity anomalies of strike limited listric fault sources based on the algorithm originally developed by Chakravarthi (2011). Fault planes are described by an exponential function to achieve numerical stability in the interpretation. The

validity and applicability of the code is demonstrated with both synthetic and real field gravity anomalies.

FORWARD GRAVITY MODELING

In a Cartesian coordinate system, let the z-axis be positive vertically downward with the x-axis transverse to the strike of the structure. The geometry of a typical listric fault structure is shown in Fig.1 (Chakravarthi, 2010; Chakravarthi, 2011). The listric fault source is having a limited strike length of 2Y along the y-axis (Fig.1). The footwall of the structure remains undeformed, and the

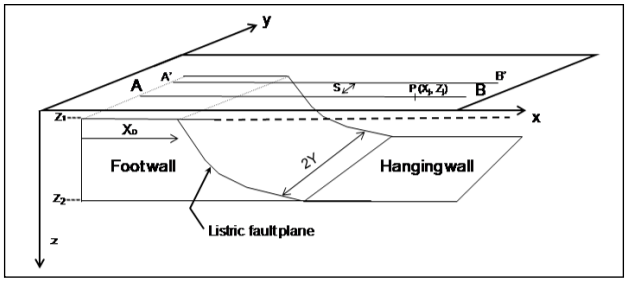

Fig.1. Schematic diagram showing geometry of a listric fault source having finite strike length.

hanging wall has been moved downward along a listric fault plane defined by a function, $\zeta(Z)$, $z_1 \le Z \le z_2$. Let the density contrast of sediments within the hanging wall vary parabolically with depth (Chakravarthi, 2003; Chakravarthi, 2011) according to

$$\Delta\rho(z)=\frac{\Delta\rho_0^3}{(\Delta\rho_0-\alpha z)^2}, \qquad (1)$$

where, $\Delta\rho_0$ is the density contrast observed at the ground surface and α is a constant. The gravity anomaly, $g_{joint}(X_j, Z_j)$, at any point, $P(X_j, Z_j)$, on the profile AB bisects the strike length of the structure is given by Chakravarthi (2011) as

$$g_{joint}(X_j, Z_j) = g_{mod}(X_j, Z_j) + \psi(X_j), \qquad (2)$$

where, $g_{mod}(X_j, Z_j)$ is the gravity effect of the listric fault source expressed by Chakravarthi (2010) as

$$g_{\mathrm{mod}}(X_j,Z_j)= 2G\Delta\rho_0^3\int_{z_1}^{z_2}\frac{1}{(\Delta\rho_0-\alpha z)^2}\left[\begin{array}{l}\tan^{-1}\dfrac{Y}{(z-Z_j)}\\ -\tan^{-1}\dfrac{Y(\zeta(z)-X_j)}{(z-Z_j)\sqrt{(\zeta(z)-X_j)^2+(z-Z_j)^2+Y^2}}\end{array}\right]dz \qquad (3)$$

and $\psi(X_j)$ is a polynomial to describe regional background,

$$\psi(X_j)=\sum_{m=0}^{2} b_m X_j^m, j = 1, 2, \ldots., N_{obs}. \qquad (4)$$

Here, z_1 and z_2 are depths to the top and bottom of the fault structure (Fig. 1), N_{obs} is number of observations on the profile, and b_m, $m = 0,1,2$ are coefficients of polynomial regional background. Chakravarthi (2011) defined the function, $\zeta(Z) = \sum_{k=0}^{NI} f_k z^k$, f_k represent the coefficients of the polynomial. However, numerical instability arises in the inversion when higher degree polynomials are chosen for the function, $\zeta(Z)$, as described by Chakravarthi (2011). Such a drawback can be overcome if the function, $\zeta(Z)$, is defined as

$$\zeta(z) = exp^{(\lambda Z + C)} \qquad (5)$$

where, λ and C are constants. In case the profile fails to bisect the strike length of the structure and runs at an offset, s, (such as the profile A'B' in Fig. 1), then the anomalies can be calculated on the profile as the average of Eq. (3) by substituting $(Y - s)$ and $(Y + s)$ for Y (Chakravarthi, 2010). The offset parameter, s, controls the magnitude of the gravity anomaly of a listric fault structure and hence this parameter plays a crucial role in modeling and inversion of gravity anomalies (Chakravarthi, 2010). It is to be noted that Eq. (2) can also be used to compute the gravity anomalies of a listric fault source using uniform density by letting α to zero.

INVERSION OF GRAVITY ANOMALIES

Inversion of gravity anomalies of a listric fault source is tantamount to a mathematical exercise of trying to fit the modeled gravity anomalies $g_{joint}(X_k, Z_k)$, $k = 1, 2, ..., N_{obs}$, to the observed anomalies, $g_{obs}(X_k, Z_k)$, and estimate the optimum parameters of the structure and coefficients of regional background, such that the modeled gravity anomalies mimic the observed ones. The inversion code presented here is automatic in the sense that it initializes both regional background and parameters of the source based on a few characteristics of the observed gravity anomaly and improves them iteratively until the modeled gravity anomalies fit the observed ones. Accordingly, the algorithm initializes regional background by fitting the polynomial, $\psi(X_j)$, to the gravity anomalies observed at stations located over the basement far away from the fault plane. The difference between the Bouguer gravity anomalies and the approximate regional is used to initialize other parameters of the structure. The approximate depth, z_2, of the structure is estimated using the Bouguer slab formula (Chakravarthi, 1995).

$$z_2 = \frac{g_{r\max}\,\Delta\rho_0}{41.89\,\Delta\rho_0^2 + \alpha\, g_{r\max}} \tag{6}$$

Here, $g_{r\max}$ is the maximum (absolute value) residual gravity anomaly on the profile. In addition, the algorithm also identifies approximate location of the fault plane, x_D, (Fig. 1) on the profile at a point at which the corresponding anomalous field reaches to one half the maximum anomaly (Murthy and Krishnamacharyulu, 1990; Murthy, 1998). Using these initial parameters the algorithm calculates the modeled gravity anomalies, $g_{joint}(X_k, Z_k)$, $k = 1, 2, ..., N_{obs}$, using Eq. (2). The difference between the observed anomalies, $g_{obs}(X_k, Z_k)$, and the modeled anomalies, $g_{joint}(X_k, Z_k)$, at any point, (X_k, Z_k), can be expressed as a cumulative effect of a truncated Taylor's series expansion involving the partial derivatives of anomaly with respect to each unknown parameter of the structure and each coefficient of the polynomial, $\psi(X_j)$, and their corresponding increments as

$$\begin{aligned} g_{obs}(X_k,Z_k) - g_{jo\,\mathrm{int}}(X_k,Z_k) = {} & \frac{\partial g_{jo\,\mathrm{int}}(X_k,Z_k)}{\partial z_1}dz_1 + \frac{\partial g_{jo\,\mathrm{int}}(X_k,Z_k)}{\partial z_2}dz_2 + \frac{\partial g_{jo\,\mathrm{int}}(X_k,Z_k)}{\partial \lambda}d\lambda \\ & + \frac{\partial g_{jo\,\mathrm{int}}(X_k,Z_k)}{\partial C}dC + \frac{\partial g_{jo\,\mathrm{int}}(X_k,Z_k)}{\partial X_D}dX_D + \sum_{m=0}^{2}\frac{\partial g_{jo\,\mathrm{int}}(X_k,Z_k)}{\partial b_m}db_m , \end{aligned} \tag{7}$$

where, dz_1, dz_2, $d\lambda$, dC, dX_D and db_m are the increments/decrements to z_1, z_2, λ, C, X_D and b_m respectively.

Linear equations similar to equation (7) are constructed for each observation on the profile and 8 normal equations are framed and solved by minimizing the quantum of misfit, J, between the observed and modeled gravity anomalies defined by

$$\sum_{k=1}^{N_{obs}}\left[g_{obs}(X_k,Z_k) - g_{jo\,\mathrm{int}}(X_k,Z_k)\right]^2 , \tag{8}$$

using ridge regression algorithm (Marquardt, 1963). The relevant system of normal equations is expressed as (Chakravarthi, 2011)

$$\begin{aligned} & \sum_{k=1}^{N_{obs}}\sum_{m=1}^{8}\frac{\partial g_{jo\,\mathrm{int}}(X_k,Z_k)}{\partial a_{j'}}\frac{\partial g_{jo\,\mathrm{int}}(X_k,Z_k)}{\partial a_m}(1+\delta_{mj'},\beta)\,da_m \\ & \quad = \sum_{k=1}^{N_{obs}}\left[g_{obs}(X_k,Z_k) - g_{jo\,\mathrm{int}}(X_k,Z_k)\right]\frac{\partial g_{jo\,\mathrm{int}}(X_k,Z_k)}{\partial a_{j'}},\ j' = 1,.....,8, \end{aligned} \tag{9}$$

where, β is damping factor. Also,

$$\begin{aligned} \delta_{mj'} &= 1 \ for\ m = j' \\ &= 0 \ for\ m \neq j' \end{aligned} ,$$

The partial derivatives required in equation (9) are calculated by a numerical method (Chakravarthi et al., 2001). The parameters of the structure are updated with the improvements, da_m, solved from equation (9) until 1) the specified number of iterations completed or 2) the misfit (equation 8) becomes less than a predefined allowable error or 3) the damping factor, β, assumes an unusually large value (Chakravarthi, 2003).

CODE

Based on the methodology described in the text GUI based JAVA code, INGRLSTRK, is developed to analyze the gravity anomalies of strike limited listric fault structures. This code is platform-independent and works on any GUI based operating system with at least jdk 1.6 version installed. The code follows *Model-View-Controller (MVC)* pattern according to the structural relationship shown in Fig. 2. The advantage of the code is that besides generating the output in both ASCII and graphical forms, it also displays in an animated form (i) the changes in model geometry, (ii) variation of each model parameter and misfit with iteration number, (iii) improvements in modeled gravity anomalies, and (iv) variation of density contrast with depth.

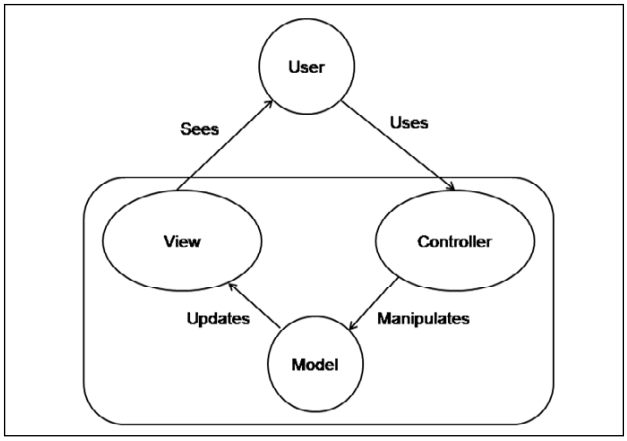

Fig.2. Structural relation between Model, View, and Controller objects.

The 'Model' initializes regional gravity background and the structure based on a few characteristics of the observed gravity anomalies as described in the text, computes model gravity anomalies of the structure and performs the business logic of the algorithm. The 'View' executes the task of displaying the results in both ASCII and graphical forms. The 'Control' performs the task of passing the required actions to the model and view modules.

The input parameters to the code consists of the area name, profile name, number of observations, distance values expressed in km, elevation values of stations in km, observed gravity anomalies in mGal, offset of the profile in km, surface density contrast in g/cm^3, alpha in g/cm^3/km, half strike length in km, maximum possible depth in km and number of iterations to be performed.

EXAMPLES

The applicability and validity of the code is demonstrated with both synthetic and real field gravity anomalies. The interpreted results are compared with assumed parameters in case of synthetic examples and with the drilling depths/ available geological information in case of real field example.

Synthetic Example

We analyze the gravity anomalies (1) solely attributing to an ideal structure having listric fault morphology with flat top and bottom surfaces, (2) solely attributing to a listric fault structure having uneven flat top and bottom surfaces with a not perfectly exponential limiting surface and (3) in the presence of both pseudorandom noise and regional gravity background.

Ideal Listric Fault Structure with Flat Top and Bottom Surfaces and Exponential Limiting Fault Plane

Noisy gravity anomalies produced by an ideal synthetic listric fault source having 50 km half-strike length (bottom panel of Fig. 3) at 45 km offset on the plane, z_j = 0, at 41 equispaced observations in the interval x [-20, 20 km] are shown as a solid line in Fig. 3a. The parameters assumed to generate the gravity anomalies of the structure are z_1=0.0001 km, z_2=10 km, X_D= 0.2599 km, λ = 0.3974, C = -1.3472 km, $\Delta\rho_0$ = -0.5206 g/cm^3 and α = 0.0574 g/cm^3/km. In this case, pseudorandom noise is Gaussian with 10% of residual signal strength. The variation of density contrast with depth within the hanging wall of the structure is shown in Fig. 3c adjacent to the assumed structure. To invert the gravity data, $\Delta\rho_0$ and α are derived based on the known density contrast-depth information (Fig. 3c), whereas half-strike length of the structure (Y) and offset distance of the profile (s) from Fig. 3b respectively. The values of $\Delta\rho_0$, α, z_1, Y and s remain unchanged, whereas the parameters z_2, X_D, λ and C are updated iteratively. The initial parameters of the structure estimated by the code are: z_2=7.9458 km, X_D= 1.005 km with the values of λ and C initially set to zero. The code performed 16 iterations before it got terminated as the misfit (J) between the observed and modeled gravity anomalies fell below a predefined allowable error of 1E-03 mGal. The estimated parameters of the structure at the end of the concluding iteration are given by z_2= 9.9 km, X_D= 0.2599 km, λ = 0.3974, C = -1.3469 km. These parameters remain more or less the same beyond the 16th iteration. The modeled gravity anomalies at the end of the 16th iteration were shown in Fig. 3a as solid dots. The fit between the observed and modeled gravity anomalies is excellent (Fig. 3a) with the estimated structure closely mimics the assumed one (Fig. 3b) even in the presence of pseudorandom noise. The error between the observed and

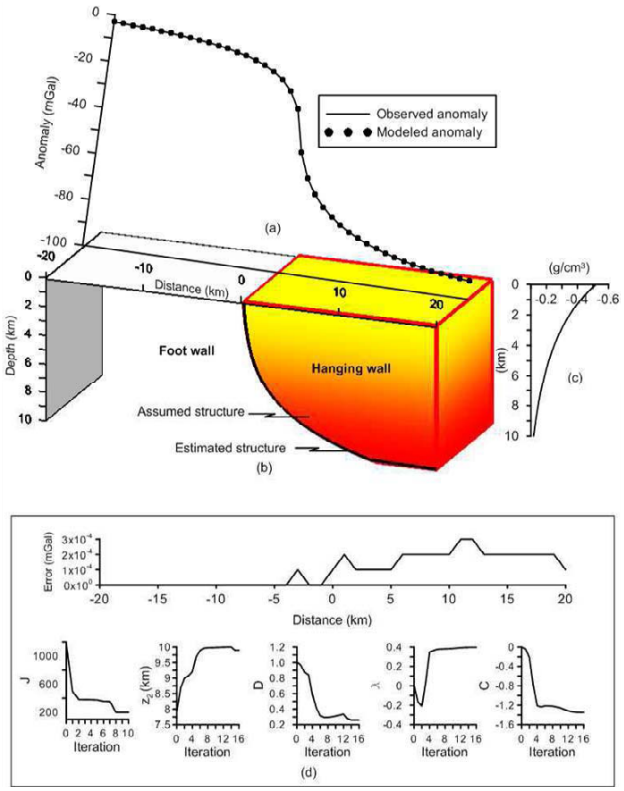

Fig.3.(a) Observed and modeled noisy gravity anomalies, **(b)** assumed and estimated listric fault structures having flat top and bottom surfaces with exponential limiting fault plane. Color gradation from yellow to red within structure indicates decrease in density contrast (absolute magnitude) with depth, **(c)** variation of density contrast within hanging wall of structure, **(d)** error analysis of the gravity anomaly along with misfit and various shape parameters versus iteration number.

modeled gravity anomalies subsequent to inversion, and changes in the parameters of the structure with iteration number are shown in Fig. 3d.

Listric Fault Structure with Uneven Top and Bottom Surfaces and Imperfect Exponential Limiting Surface

Figure 4a shows noisy gravity anomalies produced by a synthetic structure whose geometry is shown in Fig. 4b. In this case, the structure possesses variable morphological features with uneven footwall and hanging wall surfaces and imperfect exponential limiting surface. The anomalies of such a structure calculated at 20 km offset at 51equispaced observations in the interval x [-20, 30 km] are shown in Fig. 4a as a solid line. The anomalies are supplied to the code for inversion for which the code had performed 10 iterations before it got terminated as the resulting damping factor exceeds a maximum value of 12. In this case, the initial parameters of the structure estimated by the code are: z_2= 8.4524 km, X_D= -0.3742 km, with the values of λ and C initially set to zero. The modeled gravity anomalies (shown as solid dots in Fig 4a) subsequent to inversion reasonably fit the observed ones (Fig. 4a). The parameters of the structure after the inversion are given by z_2 = 9.856 km, X_D= -1.3225 km, λ = 0.5859, and C = -2.3306 km. The modeled structure moderately deviates from the assumed structure (Fig. 4b). The estimated structure portrays high angle dip for the fault plane up to a depth of 6 km, beyond which it shows moderately varying dips. In this case, the depth to hanging wall is underestimated with maximum error (12%) occur at the 12th km on the profile.

Simultaneous Estimation of Model Parameters and Regional Background

It is well-known that the process of regional and residual anomaly separation is highly subjective in the absence of known geology (Chakravarthi and Sundararajan, 2006;

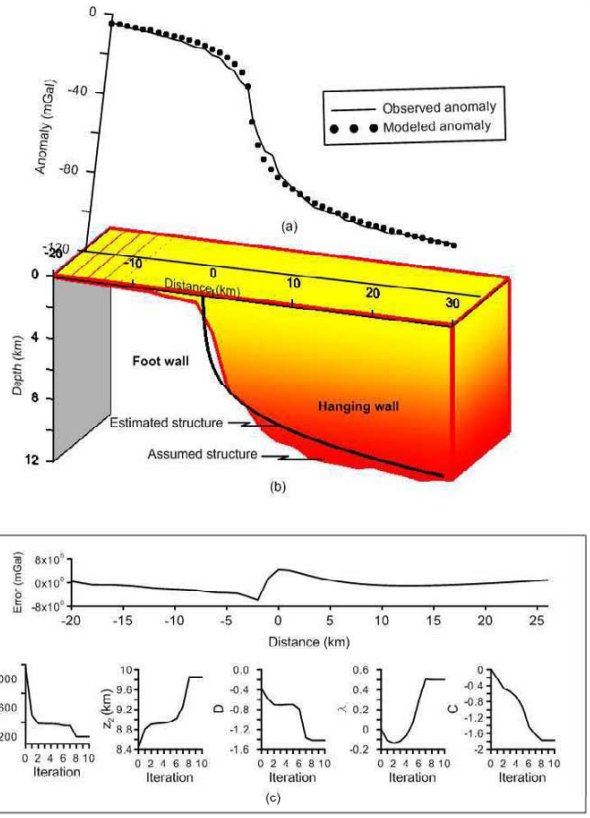

Fig.4. (a) Observed and modeled noisy gravity anomalies, **(b)** assumed listric fault structure with uneven top and bottom surfaces and imperfect exponential limiting fault plane along with the estimated structure. Colour gradation from yellow to red within structure indicates decrease in density contrast (absolute magnitude) with depth, **(c)** error analysis of the gravity anomaly along with misfit and various shape parameters versus iteration number.

Chakravarthi, 2011); hence, the degree of polynomial to be chosen to simulate regional background is always uncertain. Generally, regional gravity anomalies produced by deep-seated source/sources are characterized by long wavelength features whereas the residual anomalies generated by a shallow interfering source show shorter wavelength. Considering the characteristics of regional gravity field a 5th degree polynomial with a set of six coefficients, b_0 = -6.9113, b_1 = -0.4124, b_2 = -0.0047, b_3 = -3.4389E-5, b_4= -2.6491E-6, and b_5= 8.4231E-8 is chosen in the present case to describe the regional gravity background. This regional anomaly is then added to the noisy signal of the structure prior to inversion to study its effect on the interpretation, if any. The magnitude of assumed regional anomaly varies significantly over the length of the profile from about -0.97 mGal over the footwall to as much as -17.5 mGal over the hanging wall (Fig. 5). The combined effect of the noisy gravity anomaly and regional background is shown in Fig. 6a as solid dots.

Because the degree of polynomial to be chosen to simulate regional background is always uncertain in the absence of results by any other method including drilling, we have used a 2nd degree polynomial in the inversion to describe regional background instead of a 5th degree to study its effect. For such an inversion, the estimated initial coefficients of regional background by the algorithm are given by b_0 = -4.002, b_1 = 0.0 and b_2 = 0.0, whereas the initial parameters of the structure estimated as z_2= 10.45 km, X_D = 1.1776 km with the values of λ and C initially set to zero. For such an inversion, the code performed 23 iterations before it got terminated as no significant improvements either in model parameters or in the coefficients of regional background are found. The modeled parameters subsequent to inversion are given by

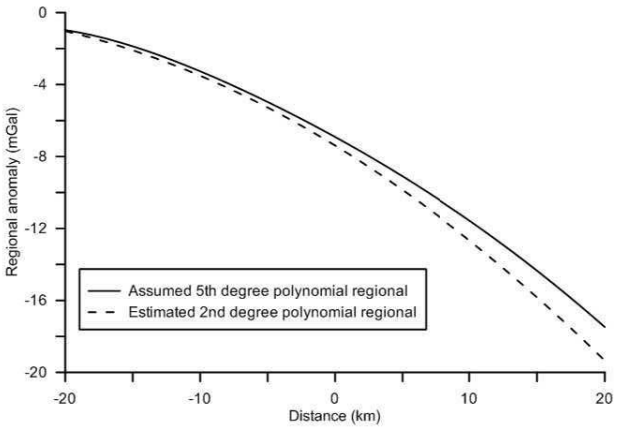

Fig.5. Assumed (5th degree polynomial) and estimated (2nd degree polynomial) regional backgrounds.

z_2= 9.44 km, X_D = 0.3712 km, λ = 0.4098, C = -1.4215 km. The modeled gravity anomalies and the estimated structure at the end of the 23rd iteration are shown in Fig. 6a and b, respectively. The fit between observed and modeled gravity anomalies is satisfactory (Fig. 6a). The inferred coefficients of the polynomial regional background at the end of 23rd iteration are given by b_0 = -7.3865, b_1= -0.4578 and b_2= -0.00699. The modeled regional background marginally deviates from the assumed regional (Fig. 5), whereas the interpreted depth to the bottom of the structure (9.44 km) is underestimated by 5.6% (Fig. 6b). Such an error between assumed and estimated depth is acceptable considering significant level of noise that is used to corrupt the gravity anomaly of the structure in the presence of a 5th degree polynomial regional background. The changes in the parameters of the structure and coefficients of regional background with iteration number are shown in Fig. 6b.

In short, in all cases the interpreted results were obtained with a possible minimum misfit between the observed and

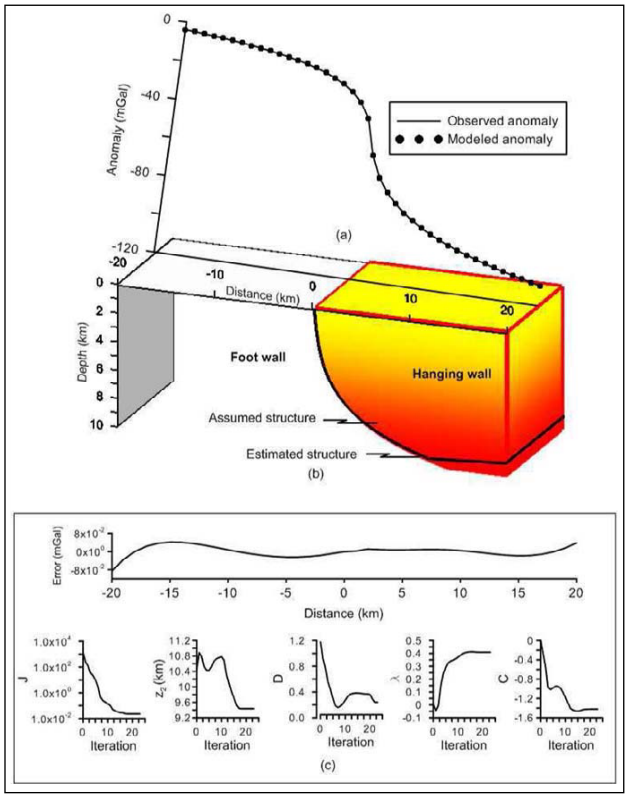

Fig.6. (a) Observed and modeled gravity anomalies in presence of regional background and pseudorandom noise, **(b)** assumed and estimated depth structures. The color gradation from yellow to red within structure indicates decrease in density contrast (absolute magnitude) with depth. **(c)** error analysis of the gravity anomaly along with misfit and various shape parameters versus iteration number.

modeled gravity responses at an amazingly very low number of iterations even in the presence of significant level of pseudorandom noise, which in turn demonstrates the efficacy of the proposed algorithm.

Field Example

Applicability and efficacy of the algorithm and code are demonstrated with the analysis of a set of observed gravity anomalies across the Aswaraopet master fault of the Chintalpudi subbasin in India. Archaean gneisses form the basement for the Gondwana sequence within the basin and the basin is bounded on the eastern side by the well-known Aswaraopet fault, which is exposed to the surface over a length of 20 km in NNW–SSE. The topography of the entire area is flat or gently undulating (Rao, 1982). The details of the gravity survey including the distribution of observations, application of various corrections to the measured data and the accuracy of Bouguer anomalies are discussed in detail by Mishra et al. (1987). Based on Deep Seismic Sounding (DSS) investigations, Kaila et al. (1990) inferred a maximum thickness of 2.8 km for the Gondwana sediments within the basin. Furthermore, the Oil and Natural Gas Corporation Ltd (ONGC), India drilled a deep borehole in the basin at its depocentre and encountered the Archaean basement at a depth of 2.935 km (Agarwal, 1995).

Chakravarthi and Sundararajan (2007) analyzed the gravity anomalies of the basin (Fig. 7a) for the 3D basement configuration using the derived parabolic density function with constants $\Delta\rho_0$ = -0.5 g/cm^3 and α = 0.1711g/cm^3/km (Fig. 7d). For the present study, the observed gravity anomalies along a profile, FF', (location is shown Fig. 7a) were analyzed using the present algorithm to quantify the Aswaraopet fault structure.

When the observed anomalies (shown as a solid line in Fig. 7b) were subjected to inversion, the code had performed 18 iterations beyond which no significant changes in the parameters of the structure and coefficients of regional anomaly were observed. The initial parameters of the structure estimated by the code are given by z_2= 2.67 km, X_D = 2.156 km with the values of λ and C initially set to zero. The modeled gravity anomalies (shown in Fig. 7b as solid dots) subsequent to inversion closely mimic the observed anomalies (Fig. 7b). The estimated parameters of the structure after the inversion are given by z_2= 2.99 km, X_D = 0.7529 km, λ = 0.7289, C = -0.2845 km. The estimated coefficients of regional background are given by b_0 = -0.4526, b_1 = -0.0658, and b_2 = -0.0104673 and shown graphically in Fig. 7b. The fact that the estimated thickness of sediments from the present method (2.99 km) corroborates well both with the drilling information (2.935 km) as well as the DSS results (2.8 km) demonstrates the applicability and efficacy of the method.

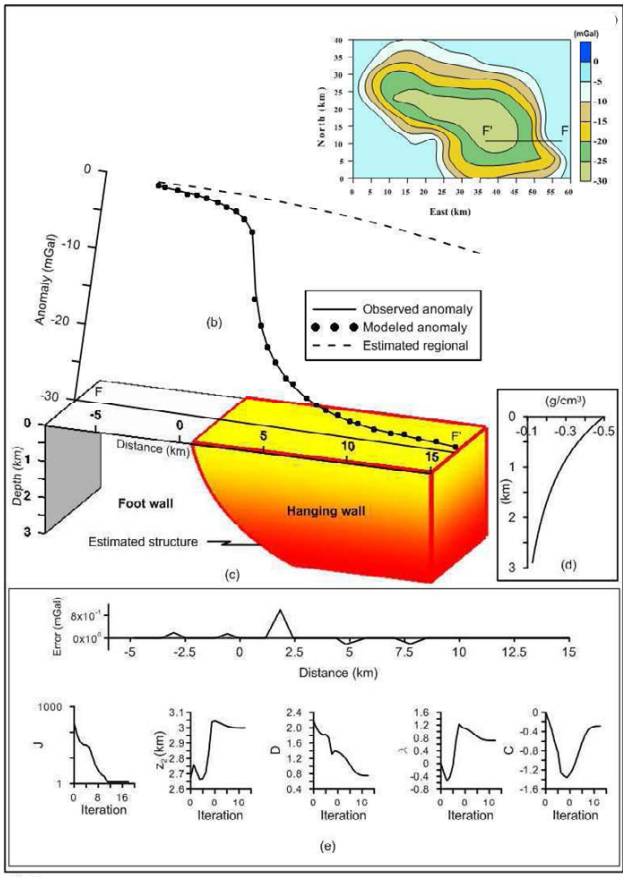

Fig.7. (a) Observed gravity anomaly map, Chintalpudi subbasin, India (Chakravarthi and Sundararajan, 2007). Interpretation has been carried out along a profile FF'. **(b)** Observed, modeled gravity anomalies and estimated regional gravity background, **(c)** estimated depth structure. The color gradation from yellow to red within structure indicates decrease in density contrast (absolute magnitude) with depth, **(d)** variation of density contrast with depth, **(e)** error analysis of the gravity anomaly along with misfit and various shape parameters versus iteration number.

CONCLUSIONS

An automatic method and associated code, INGRLSTRK, are developed to analyze the gravity anomalies of strike limited listric fault structures and regional gravity background from observed Bouguer gravity anomalies. The novelty of the method is that it generates the results not only in graphical form but also displays in animation.

The validity and applicability of the code is demonstrated on both ideal and non-ideal synthetic listric fault

morphologies. When the noisy anomalies of an ideal structure with a flat top and a bottom surfaces are analyzed, the estimated structure closely mimics the assumed one, whereas in case of non-ideal structure with uneven top and bottom surfaces with imperfect exponential limiting surface, the estimated structure moderately deviated from the assumed structure. Further, in the presence of both regional background and pseudorandom noise the estimated structure modestly deviated from the assumed structure with the depth of the structure is marginally underestimated by 5.6%. The analysis of observed gravity anomalies along a profile across the Aswaraopet master fault of the Chintalpudi subbasin in India has yielded information that is consistent with both DSS results and drilling information.

However, the method has certain limitations. In the derivation of gravity expression of the structure it is assumed that (i) the foot wall of the structure remains intact and undisturbed and the base of the hanging wall is flat, and (ii) regional gravity background varies according to a 2^{nd} degree polynomial. Elsewhere, the regional background may not be exactly simulated by a 2^{nd} degree polynomial because the degree of the polynomial to be chosen is uncertain in the absence of known geology. We conclude that the proposed strategy is more effective in geological settings where the enlisted assumptions are more or less valid. The advantage of the proposed method is that it can be used to analyze the gravity anomalies of the structure even when the profile along which interpretation is intended fails to bisect the strike length of the structure.

Acknowledgements: The authors sincerely thank the anonymous reviewers for their excellent reviews and feedback to improve the quality of the manuscript as presented.

References

AGARWAL, B.P. (1995) Hydrocarbon prospects of the Pranhita-Godavari graben, India. *In:* Petrotech-95 proceedings of the first International petroleum conference exhibition, Hyderabad, India. pp.115–121.

BHASKARA RAO, D. (1985) Analysis of gravity anomalies over an inclined fault with quadratic density function. Pure and Applied Geophysics, v.123 (2), pp.250–260.

BHASKARA RAO, D., PRAKASH, M.J. and RAMESH BABU, N. (1993) Gravity interpretation using Fourier transforms and simple geometrical models with exponential density contrast. Geophysics, v.58, pp.1074–1083.

BRADY, R., WERNICKE, B. and FRYXELL, J. (2000) Kinematic evolution of a large-offset continental normal fault system; South Virgin Mountains, Nevada. Geol. Soc. Amer. Bull., v. 112, pp.1375-1397.

CHAKRAVARTHI, V. (1995) Gravity interpretation of nonoutcropping sedimentary basins in which the density contrast decreases parabolically with depth. Pure and Applied Geophysics, v.145, pp.327–335.

CHAKRAVARTHI, V. (2003) Digitally implemented method for automatic optimization of gravity fields obtained from three-dimensional density interfaces using depth dependent density. US Patent 6,615,139.

CHAKRAVARTHI. V. (2008) Gravity inversion of 2.5D faulted beds using depth dependent density. Curr. Sci., v.95, pp.1618-1622.

CHAKRAVARTHI, V. (2010) LSTRKFALTG — A forward modeling program to compute theoretical gravity anomalies of strike limited listric fault structures with prescribed vertical variation in density. Computers & Geosciences, v.36 (5), pp.675–679.

CHAKRAVARTHI, V. (2011) Automatic gravity optimization of 2.5D strike listric fault sources with analytically defined fault planes and depth-dependent density. Geophysics, v.76(2), pp. I21-I31.

CHAKRAVARTHI, V., SINGH, S.B. and ASHOK BABU, G. (2001) INVER2DBASE — A program to compute basement depths of density interfaces above which the density contrast varies with depth. Computers & Geosciences, v.27, pp.1127–1133.

CHAKRAVARTHI, V. and SUNDARARAJAN, N. (2004) Ridge regression algorithm for gravity inversion of fault structures with variable density. Geophysics, v.69, pp.1394–1404.

CHAKRAVARTHI, V. and SUNDARARAJAN, N. (2006) Gravity anomalies of 2.5-D multiple prismatic structures with variable density: a Marquardt inversion. Pure and Applied Geophysics, v.163, pp.229–242.

CHAKRAVARTHI, V. and SUNDARARAJAN, N. (2007) 3D gravity inversion of basement relief – A depth dependent density approach. Geophysics, v.72, pp.123-132.

CHAPPELL, A. and KUSZNIR, N. (2008) An algorithm to calculate the gravity anomaly of sedimentary basins with exponential density-depth relationships. Geophysical Prospecting, v.56 (2), pp.249–258.

CHEN, W., ZHANG, S. and SHI, Y. (1992) An effective method of fault gravity inversion. Jour. Nanjing Univ., v.4(1), pp.68–74.

CORDELL, L. (1973) Gravity anomalies using an exponential density-depth function -San Jacinto Graben, California. Geophysics, v.38, pp.684–690.

GARCÍA-ABDESLEM, J. (2000) 2-D inversion of gravity data using sources laterally bounded by continuous surfaces and depth-dependent density. Geophysics, v.65(4), pp.1128–1141.

GIMENEZ, M. E., MARTINEZ, M. P., JORDAN, T., RUÍZ, F. and LINCE KLINGER, F. (2009) Gravity characterization of the La Rioja Valley basin, Argentina. Geophysics, v.74(3), pp.B83–B94.

JACKSON, J. A. (1987) Active normal faulting and crustal extension. Geol. Soc. London Spec. Publ., v.28, pp.3–17.

Jackson, J.A. and McKenzie, D. (1983) The geometrical evolution of normal fault systems. Jour. Struc. Geol., v.5, pp.471-482.

Janecke, S.U., Vandenburg, C.J. and Blankenau, J.J. (1998) Geometry, mechanisms and significance of extensional folds from examples in the Rocky Mountain Basin and Range province, U.S.A. Jour. Struc. Geol., v.20, pp.841-856.

Kaila, K.L., Murthy, P.R.K., Rao, V.K. and Venkateswarlu, N. (1990) Deep seismic sounding in the Godavari Graben and Godavari (Coastal) Basin, India. Tectonophysics, v.173, pp.307-317.

Li, X. (2001) Vertical resolution: Gravity versus vertical gravity gradient. The Leading Edge, v.20, pp.901–904.

Martín-Atienza, B. and García-Abdeslem, J. (1999) 2-D gravity modeling with analytically defined geometry and quadratic polynomial density functions. Geophysics, v.64, pp.1730–1734.

Marquardt, D. W. (1963) An algorithm for least squares estimation of nonlinear parameters: Journal Society Indian Applied Mathematics, v.11, pp.431–441.

McKenzie, D. (1978) Some remarks on the development of sedimentary basins. Earth Planet. Sci. Lett., v.40, pp.25-32.

Mishra, D.C., Gupta, S.B., Rao, M.B.S.V., Venkatarayudu, M. and Laxman, G. (1987) Godavari basin – a geophysical study. Jour. Geol. Soc. India, v.30, pp.469-476.

Murthy, I.V.R. (1998) Gravity and magnetic interpretation in Exploration Geophysics: Geological Society of India, Bangalore, 363p.

Murthy, I.V.R. and Krishnamacharyulu, S.K.G. (1990) Automatic inversion of gravity anomalies of faults: Computers & Geosciences, v.16, pp.539-548.

Pawlowski, R. (2008) The use of gravity anomaly data for offshore continental margin demarcation. The Leading Edge, v.27, pp.722–727.

Peirce, J.W. and Lipkov, L. (1988) Structural interpretation of the Rukwa rift, Tanzania. Geophysics, v.53, pp.824–836.

Rao, C. S. R. (1982) Coal resources of Tamil Nadu, Andhra Pradesh, Orissa and Maharashtra. Bull. Geol. Surv. India, v.2, pp.1–103.

Stavrev, P. and Reid, A. (2010) Euler deconvolution of gravity anomalies from thick contact/fault structures with extended negative structural index. Geophysics, v.75, pp.I51-I58.

Sundararajan, N. and Ramabrahmam, G. (1998) Spectral analysis of gravity anomalies caused by slab-like structures: A Hartley transform technique. Journal of Applied Geophysics, v.39(1), pp.53–61.

Thanassoulas, C., Tselentis, G.A. and Dimitriadis, K. (1987) Gravity inversion of a fault by Marquardt's method. Computers & Geosciences, v.1(4), pp.399–404.

Torizin, J., Jentzsch, G., Malischewsky, P., Kley, J., Abakanov, N. and Kurskeev, A. (2009) Rating of seismicity and reconstruction of the fault geometries in northern Tien Shan within the project "Seismic Hazard Assessment for Almaty". Jour. Geodynamics, v.48 (3–5), pp.269–278.

Wernicke, B. and Burchfiel, B.C. (1982) Modes of extensional tectonics. Journal of Structural Geology, v. 4, pp. 105–115.

Zhang, J., Zhong, B., Zhou, X. and Dai, Y. (2001) Gravity anomalies of 2-D bodies with variable density contrast. Geophysics, v.66, pp.809–813.

Zhou, X. (2008) 2D vector gravity potential and line integrals for the gravity anomaly caused by a 2D mass of depth-dependent density contrast. Geophysics, v.73(6), pp.143-150

Zhou, X. (2009) General line integrals for gravity anomalies of irregular 2D masses with horizontally and vertically dependent density contrast. Geophysics, v. 74 (2), pp. 11-17.

(Received: 8 January 2013; Revised form accepted: 17 April 2013)